complexes has been confirmed by X-ray structural determination on compound 9.[21] The spectroscopic properties of 9–11 (Table I) are consistent with their formulation: one hydride chemical shift at −10 to −12 ppm (δ value) in the ^{1}H NMR, three different chemical shifts for the phosphorus atoms in the ^{31}P NMR, and a ν(NO) stretching between 1630–1665 cm^{-1}. The three different phosphorus atoms can be differentiated from one another without ambiguity: only two-bond phosphorus–phosphorus couplings are resolved, and one-bond phosphorus–hydrogen coupling (9, 349; 10, 352; 11, 350 Hz) is characteristic for Ph_2PH. The assymmetric nature of these complexes is most clearly seen from the presence of diastereometric methylene protons in 9. The successful synthesis of 9–11 nicely illustrated the crucial role of the diphosphine ligands in retaining the dimeric metal unit as frequently observed[22] and the NO ligand in activating the coordinated CO ligand.[23] The chemical reactivity of the complexes 1–6 will be pursued further and be reported in due course.

Acknowledgment. We wish to thank the National Science Council of Republic of China for the support (Grant NSC 79-0208-M001-07).

Supplementary Material Available: Listings of all bond distances and angles, anisotropic thermal parameters and isotropic thermal parameters, and positional parameters for calculated hydrogen atoms for compounds 1, 3, 7, and 8 (23 pages); listings of structure factors (91 pages). Ordering information is given on any current masthead page.

(21) Lin, J. T.; Chang, K. Y. Unpublished results. Orange crystals of 9 were grown by cooling a concentrated solution of 9 in CH_3CN. Crystal data: orthorhombic, space group *Pbca*, a = 19.408 (5), b = 36.100 (8), c = 12.025 (1) Å.

(22) (a) Blagg, A.; Robson, R.; Shaw, B. L.; Thornton-Pett, M. *J. Chem. Soc., Dalton Trans.* **1987**, 2171. (b) Jacobsen, G. B.; Shaw, B .L.; Thornton-Pett, M. *J. Chem. Soc., Dalton Trans.* **1987**, 1509. (c) Ibid. Jacobsen, G. B.; Shaw, B. L.; Thornton-Pett, M. *J. Chem. Soc., Dalton Trans.* **1987**, 1489.

(23) Richter-Addo, G. B.; Legzdins, P. *Chem. Rev.* **1988**, *88*, 1010.

Isomerism in 47- and 48-Electron (Methylidyne)triruthenium Clusters. Crystal Structures[1] of $(\mu\text{-H})_3Ru_3(\mu_3\text{-COMe})(CO)_6\{\mu_3\text{-}(PPh_2CH_2)_3CMe\}$ and $(\mu\text{-H})_3Ru_3(\mu_3\text{-COMe})(CO)_7\{\mu_2\text{-}(PPh_2)_3CH\}\cdot 1.25CH_2Cl_2$

Melvyn Rowen Churchill,* Charles H. Lake, William G. Feighery, and Jerome B. Keister*

Department of Chemistry, University at Buffalo, State University of New York, Buffalo, New York 14214

Received January 8, 1991

Ligand substitution on $(\mu\text{-H})_3Ru_3(\mu_3\text{-COMe})(CO)_9$ has been used to prepare the clusters $(\mu\text{-H})_3Ru_3(\mu_3\text{-COMe})(CO)_6\{\mu_3\text{-}(PPh_2CH_2)_3CMe\}$ and $(\mu\text{-H})_3Ru_3(\mu_3\text{-COMe})(CO)_7\{\mu_2\text{-}(PPh_2)_3CH\}$. The complex $(\mu\text{-H})_3Ru_3(\mu_3\text{-COMe})(CO)_6\{\mu_3\text{-}(PPh_2CH_2)_3CMe\}$ crystallizes in the centrosymmetric triclinic space group $P\bar{1}$ with a = 10.053 (2) Å, b = 12.920 (3) Å, c = 19.185 (4) Å, α = 87.23 (2)°, β = 75.80 (2)°, γ = 77.62 (2)°, V = 2359.6 (9) Å^3, and Z = 2. The molecule has approximate C_3 symmetry, with the μ_3-COMe group and the μ_3-$MeC(CH_2PPh_2)_3$ ligand capping opposite faces of the planar triruthenium core; the P-donor atoms thus are all in axial sites. Electrochemical and chemical oxidation of $(\mu\text{-H})_3Ru_3(\mu_3\text{-COMe})(CO)_6\{\mu_3\text{-}(PPh_2CH_2)_3CMe\}$ forms the corresponding 47-electron radical cation, characterized by EPR spectroscopy. The complex $(\mu\text{-H})_3Ru_3(\mu_3\text{-COMe})(CO)_7\{\mu_2\text{-}(PPh_2)_3CH\}$ crystallizes from CH_2Cl_2 in the centrosymmetric monoclinic space group $P2_1/n$ with a = 21.653 (6) Å, b = 19.078 (4) Å, c = 25.238 (8) Å, β = 106.63 (3)°, V = 9989 (5) Å^3, and Z = 8. The crystallographic asymmetric unit contains 2 triruthenium cluster molecules and 2.5 CH_2Cl_2 molecules. The $(PPh_2)_3CH$ ligand behaves only as a bidentate bridging ligand and spans adjacent equatorial sites on two ruthenium atoms.

Introduction

Recently the importance of redox processes in organometallic chemistry has become apparent.[2] Of particular interest are the redox properties of transition-metal cluster compounds, which can in principle display a wide range of oxidation states. A number of electrochemical studies have focused upon clusters containing a triangular metal core capped by a main-group atom.[3-8] Many of these

(1) Structural Studies on Ruthenium Carbonyl Hydrides. 16. Part 15: Churchill, M. R.; Buttrey, L. A.; Keister, J. B.; Ziller, J. W.; Janik, T. S.; Striejewske, W. S. *Organometallics* **1990**, *9*, 766.

(2) (a) Tyler, D. R. *Prog. Inorg. Chem.* **1988**, *36*, 125. (b) Kochi, J. K. *J. Organomet. Chem.* **1986**, *300*, 139. (c) Connelly, N. G. *Chem. Soc. Rev.* **1989**, *18*, 153. (d) Geiger, W. E. *Prog. Inorg. Chem.* **1985**, *33*, 275. (e) Connelly, N. G.; Geiger, W. E. *Adv. Organomet. Chem.* **1985**, *24*, 87. (f) Drake, S. R. *Polyhedron* **1990**, *9*, 455.

(3) (a) Wei, C. H.; Dahl, L. F. *Inorg. Chem.* **1967**, *6*, 1229. (b) Strouse, C. E.; Dahl, L. F. *J. Am. Chem. Soc.* **1971**, *93*, 6032. (c) Honrath, U.; Vahrenkamp, H. *Z. Naturforsch.* **1984**, *39B*, 555.

(4) (a) Peake, B. M.; Robinson, B. H.; Simpson, J.; Watson, D. J. *Inorg. Chem.* **1977**, *16*, 405. (b) Bond, A. M.; Peake, B. M.; Robinson, B. H.; Simpson, J.; Watson, D. J. *Inorg. Chem.* **1977**, *16*, 410. (c) Bond, A. M.; Dawson, P. A.; Peake, B. M.; Rieger, P. H.; Robinson, B. H.; Simpson, J. *Inorg. Chem.* **1979**, *18*, 1413. (d) Downard, A. J.; Robinson, B. H.; Simpson, J. *Organometallics* **1986**, *5*, 1122. (e) Kotz, J. C.; Petersen, J. V.; Reed, R. C. *J. Organomet. Chem.* **1976**, *120*, 433.

0276-7333/91/2310-2384$02.50/0

clusters undergo reversible one-electron reductions to the corresponding 49-electron radical anions. Fewer examples of reversible oxidations to 47-electron radical cations have been found.[6d,7,9]

We recently reported the 47-electron clusters $[H_3Ru_3(\mu_3\text{-}CX)(CO)_6(PPh_3)_3]^+$ (X = NMeBz, SEt, OMe), generated by chemical or electrochemical oxidations of the 48-electron neutral analogues.[10] Although all of the tris(triphenylphosphine) 48-electron derivatives have equivalent, axially coordinated phosphine ligands, for X = OMe, oxidation was accompanied by isomerization to a structure having very low symmetry. Possibilities for the isomerization process were (1) axial–equatorial phosphine ligand rearrangement and (2) hydride or COMe ligand migrations.

To test the first possibility, we sought to prepare a trisubstituted derivative in which axial–equatorial ligand rearrangement was prevented by chelation of a tridentate triphosphine ligand to the Ru_3 face. Toward this end we reacted $H_3Ru_3(COMe)(CO)_9$ with two such potentially tridentate ligands, $(PPh_2CH_2)_3CMe$ and $(PPh_2)_3CH$. We report the structures of the products from these reactions, $(\mu\text{-}H)_3Ru_3(\mu_3\text{-}COMe)(CO)_6\{\mu_3\text{-}(PPh_2CH_2)_3CMe\}$, which has the desired face-capped structure, and $(\mu\text{-}H)_3Ru_3(\mu_3\text{-}COMe)(CO)_7\{\mu_2\text{-}(PPh_2)_3CH\}$, an unusual example of equatorial substitution in this class of clusters; also described are the electrochemical and chemical oxidations of $(\mu\text{-}H)_3Ru_3(\mu_3\text{-}COMe)(CO)_6\{\mu_3\text{-}(PPh_2CH_2)_3CMe\}$ to the corresponding 47-electron radical cation.

Experimental Section

Physical Methods of Characterization. Infrared spectra were recorded on a Mattson Instruments Alpha Centauri FTIR instrument or a Beckman 4250 spectrophotometer (calibrated with use of the 2138.5-cm^{-1} absorption for cyclohexane) in dichloromethane solution. Proton NMR spectra were obtained on a JEOL FX-90, a Varian Associates Gemini 300, or a Varian Associates VXR-400S instrument using chloroform-*d* or dichloromethane-d_2 as solvent and TMS as reference. Carbon NMR spectra were recorded either on the Gemini 300 or the VXR-400S instrument using chloroform-*d* as solvent and TMS as reference. Phosphorus NMR spectra were recorded on the VXR-400S instrument using chloroform-*d* as solvent, and chemical shifts are reported relative to o-phosphoric acid. EPR spectra were recorded on an IBM/Bruker X-band ER-200 SRC spectrometer, with a microwave power of 20 mW, in dichloromethane solution at room temperature.[11]

Syntheses. $H_3Ru_3(COMe)(CO)_6\{(PPh_2CH_2)_3CMe\}$. To a solution of $H_3Ru_3(COMe)(CO)_9$[12] (80 mg) in 20 mL of CH_2Cl_2 was added 83 mg (1 equiv) of $(PPh_2CH_2)_3CMe$. This solution was refluxed under nitrogen for 48 h. The solvent was removed and the product washed twice with 10 mL of ether. A light yellow solid, insoluble in ether, remained. This was recrystallized from a CH_2Cl_2/CH_3OH solution. The yield of $H_3Ru_3(COMe)(CO)_6\{(PPh_2CH_2)_3CMe\}$ was 77 mg (51%). Anal. Calcd for $Ru_3C_{49}H_{45}O_7P_3$: C, 51.53; H, 3.97. Found: C, 51.67; H, 3.92. ^1H NMR ($CDCl_3$): 7.80 (br, 6 H), 7.50 (br, 9 H), 7.22 (br, 9 H), 6.58 (br, 6 H), 4.05 (s, 3 H, OCH_3), 2.46 (dm, 6 H, CH_2), 1.37 (br, 3 H, CH_3), −16.89 (t, 3 H, J_{PH} = 22.5 Hz, RuHRu) ppm. $^{31}P\{^1H\}$ NMR ($CDCl_3$): 31.2 ppm. IR (CH_2Cl_2): 2030 (s), 2015 (vs), 1952 (m) cm^{-1}. EI MS: m/z 1144 ($^{102}Ru_3$).

$H_3Ru_3(COMe)(CO)_7\{(PPh_2)_3CH\}$. To a stirred solution of 157 mg of $H_3Ru_3(COMe)(CO)_9$[12] in 20 mL of CH_2Cl_2 was added 148 mg (1 equiv) of $(PPh_2)_3CH$. This solution was refluxed overnight. The mixture was separated by thin-layer chromatography on silica, with dichloromethane as eluent. The bottom orange band was extracted and was recrystallized from CH_2Cl_2/CH_3OH to give 253 mg of product (89% yield). The sample was stored under vacuum overnight before submission for analysis. Anal. Calcd for $Ru_3C_{46}H_{37}O_8P_3$: C, 49.60; H, 3.35. Found: C, 49.76; H, 3.13. ^1H NMR ($CDCl_3$): 7.2 (br m, 30 H), 5.52 (t, 1 H, J_{PH} = 17 Hz), 4.12 (s, 3 H, OMe), −16.77 (m, 2 H, RuHRu, J_{PH} = 25 Hz, $J_{P'H}$ = 14 Hz), −17.57 (tt, 1 H, RuHRu, J_{PH} = 13.8 Hz, J_{HH} = 2.5 Hz) ppm. ^{13}C NMR ($CDCl_3$): 67.8 (1 C, s, OCH_3), 137.4 (1 C, t, J_{PC} = 27 Hz, P_3CH), 193.1 (1 C, s, axial CO on $Ru(CO)_3$), 193.9 (2 C, t, J_{PC} = 7 Hz, axial or equatorial CO's on $Ru(CO)_2P$), 195.2 (2 C, t, J_{PC} = 5.3 Hz, axial or equatorial CO's on $Ru(CO)_2P$), 199.2 (2 C, s, equatorial CO on $Ru(CO)_3$), 260.1 (1 C, t, J_{PC} = 3.5 Hz, μ_3-C), 127–136 (36 C, phenyl carbons) ppm. $^{31}P\{^1H\}$ NMR ($CDCl_3$): 2.36 (1 P), 50.86 (2 P) ppm. IR (CH_2Cl_2): 2071 m, 2012 s, 1988 m, 1964 w, 1958 w cm^{-1}.

Electrochemistry. Cyclic voltammetric experiments were performed with a BAS-100 electrochemical analyzer. The working electrode was a 3-mm platinum-disk electrode, and the auxiliary electrode was a platinum wire. The reference electrode was the SCE. Dichloromethane was freshly distilled from calcium hydride and stored under nitrogen. The supporting electrolyte was 0.1 M tetrabutylammonium tetrafluoroborate. The concentration of the cluster was 10^{-3} M, and a nitrogen purge was mantained to exclude oxygen. Compensation for *iR* drop was employed for these measurements, and under these conditions ferrocene exhibited a reversible couple at 0.53 V (ΔE = 60 mV).

Low-Temperature EPR Spectroscopy of $H_3Ru_3(COMe)(CO)_6\{(PPh_2CH_2)_3CMe\}$. A Schlenk flask containing a stirred solution of 30 mg of $H_3Ru_3(COMe)(CO)_6\{(PPh_2CH_2)CMe\}$ in 10 mL of dry dichloromethane under nitrogen was placed in a dry ice/acetone bath. One equivalent (6.7 mg) of $AgSO_3CF_3$ was added. The solution was stirred for approximately 1 min, after which time it was filtered into an EPR tube, which was cooled in a dry ice/acetone bath under nitrogen, with great care to ensure that the solution remained cold and was under nitrogen. The green solution of the radical was evident as the EPR tube was transferred to a liquid-nitrogen bath and was vacuum-sealed. The EPR tube was kept in liquid nitrogen until the temperature of the spectrometer reached 200 K. At this time the tube was warmed gradually in a dry ice/acetone bath before being placed in the spectrometer.

Collection of X-ray Diffraction Data and Solution of the Crystal Structures. Crystals were sealed in thin-walled glass capillaries and aligned on a Siemens R3m/V diffractomer, by the methods outlined previously.[13]

All crystallographic calculations were carried out on a VAX3100 workstation with use of the Siemens SHELXTL PLUS program set. Analytical scattering factors for neutral atoms were corrected for the $\Delta f'$ and $i\Delta f''$ components of anomalous disposion. Hydrogen atoms were included in idealized positions with d(C–H) = 0.96 Å.[14]

1. **$(\mu\text{-}H)_3Ru_3(\mu_3\text{-}COMe)(CO)_6\{\mu_3\text{-}(PPh_2CH_2)_3CMe\}$.** This species crystallizes in the triclinic crystal system, in the centrosymmetric space group $P\bar{1}$. The structural analysis was associated with no unusual problems. Details appear in Table I. Final atomic coordinates are provided in Table II.

2. **$(\mu\text{-}H)_3Ru_3(\mu_3\text{-}COMe)(CO)_7\{\mu_2\text{-}(PPh_2)_3CH\}\cdot 1.25CH_2Cl_2$.** The species crystallizes in the monoclinic system. The systematic absences $h0l$ for $h + l = 2n + 1$ and $0k0$ for $k = 2n + 1$ uniquely define the centrosymmetric monoclinic space group $P2_1/n$.

Unlike the previous structural analysis, this study was accom-

(5) (a) Lindsay, P. N.; Peake, B. M.; Robinson, B. H.; Simpson, J.; Honrath, U.; Vahrenkamp, H.; Bond, A. M. *Organometallics* **1984**, *3*, 413. (b) Honrath, U.; Vahrenkamp, H. *Z. Naturforsch.* **1984**, *39B*, 545.

(6) (a) Bedard, R. L.; Rae, A. D.; Dahl, L. F. *J. Am. Chem. Soc.* **1986**, *108*, 5924. (b) Bedard, R. L; Dahl, L. F. *J. Am. Chem. Soc.* **1986**, *108*, 5933. (c) Bedard, R. L.; Dahl, L. F. *J. Am. Chem. Soc.* **1986**, *108*, 5942. (d) Ziebarth, M. S.; Dahl, L. F. *J. Am. Chem. Soc.* **1990**, *112*, 2411.

(7) Enoki, S.; Kawamura, T.; Yonezawa, T. *Inorg. Chem.* **1983**, *22*, 3821.

(8) Ohst, H. H.; Kochi, J. K. *Inorg. Chem.* **1986**, *25*, 2066.

(9) Connelly, N. G.; Forrow, N. J.; Knox, S. A. R.; Macpherson, K. A.; Orpen, A. G. *J. Chem. Soc., Chem. Commun.* **1985**, 16.

(10) Feighery, W. G.; Allendoerfer, R. D.; Keister, J. B. *Organometallics* **1990**, *9*, 2424.

(11) For a more detailed account of the EPR experiment, see: Male, R.; Samotowka, M. A.; Allendoerfer, R. D. *Electroanalysis* **1989**, *1*, 333.

(12) Keister, J. B.; Payne, M. W.; Muscatella, M. J. *Organometallics* **1983**, *2*, 219.

(13) Churchill, M. R.; Lashewycz, R. A.; Rotella, F. J. *Inorg. Chem.* **1977**, *16*, 265.

(14) Churchill, M. R. *Inorg. Chem.* **1973**, *12*, 1213.

Table I. Crystallographic Data for $(\mu\text{-H})_3Ru_3(\mu_3\text{-COMe})(CO)_6\{\mu_3\text{-}(PPh_2CH_2)_3CMe\}$ and $(\mu\text{-H})_3Ru_3(\mu_3\text{-COMe})(CO)_7\{\mu_2\text{-}(PPh_2)_3CH\}\cdot 1.25CH_2Cl_2$

	μ_3-$(PPh_2CH_2)_3CMe$ complex	μ_2-$(PPh_2)_3CH$ complex
	Crystal Data	
empirical formula	$C_{49}H_{45}O_7P_3Ru_3$	$C_{46}H_{37}O_8P_3Ru_3\cdot 1.25CH_2Cl_2$
color	yellow	orange
cryst size, mm	0.20 × 0.17 × 0.25	0.3 × 0.35 × 0.25
cryst syst	triclinic	monoclinic
space group	$P\bar{1}$	$P2_1/n$
unit cell dimens		
a, Å	10.053 (2)	21.653 (6)
b, Å	12.920 (3)	19.078 (4)
c, Å	19.185 (4)	25.238 (8)
α, deg	87.23 (2)	90
β, deg	75.80 (2)	106.63 (3)
γ, deg	77.62 (2)	90
V, Å^3	2359.6 (9)	9989 (5)
Z	2	8
fw	1142.0	1215.9
density (calcd), Mg/m^3	1.607	1.617
abs coeff, mm^{-1}	1.078	1.148
F(000)	1144	4384
	Data Collection	
diffractometer used	Siemens R3m/V	
radiation	Mo Kα (λ = 0.710 73 Å)	
temp, K	298	
monochromator	high oriented graphite cryst	
2θ range, deg	5.0–45.0°	5.0–40.0
scan type	2θ–θ	2θ–θ
scan speed, deg/min	constant; 1.50 in ω	constant; 8.08 in ω
scan range (ω), deg	0.45 plus Kα separation	0.27 plus Kα separation
bkgd measurement	stationary cryst and stationary counter at scan and end of scan, each for 25.0% of total scan time	
std rflns	3 measd every 97 rflns	3 measd every 147 rflns
index ranges	$0 \le h \le 10, -13 \le k \le 13, -20 \le l \le 20$	$0 \le h \le 20, 0 \le k \le 18, -24 \le l \le 23$
no. of rflns collected	6716	12 458
no. of indep rflns	6193 (R_{int} = 1.29%)	9358 (R_{int} = 6.25%)
no. of obsd rflns	4276 ($F > 6.0\sigma(F)$)	5264 ($F > 6.0\sigma(F)$)
abs cor	semiempirical	semiempirical
min/max transmissn	0.8242/0.9496	0.6316/0.7836
	Solution and Refinement	
system used	Siemens SHELXTL PLUS (VMS)	
soln	direct methods	
refinement method	full-matrix least squares	
quantity minimized	$\sum w(F_o - F_c)^2$	
extinction cor[a]	χ = 0.000 04 (4)	χ = 0.000 007 (14)
H atoms[b]	Riding model, fixed isotropic U	
weighting scheme	$w^{-1} = \sigma^2(F) + 0.0011F^2$	$w^{-1} = \sigma^2(F) + 0.0059F^2$
no. of params refined	569	730
final R indices (obsd data), %	R = 3.13, R_w = 3.47	R = 5.51, R_w = 7.48
R indices (all data), %	R = 5.62, R_w = 4.93	R = 9.80, R_w = 10.66
goodness of fit	1.16	0.90
largest and mean Δ/σ	0.033, 0.011	0.081, 0.006
data to param ratio	7.6:1	7.4:1
largest diff peak, e/Å^3	0.59	1.11
largest diff hole, e/Å^3	−0.46	0.79

[a] $F^* = F[1 + 0.002\chi F^2/(\sin 2\theta)]^{-1/4}$. [b] Positional parameters for the hydride ligands were refined.

panied by substantial problems. The first few crystals examined (size ~0.1 × 0.1 × 0.1 mm) were severely affected by exposure to the X-ray beam (even though the crystals appear to be stable in the air!). Examination showed definite signs of decomposition, with brownish deposits inside the capillary surrounding the site of the crystal. Finally, we selected a much larger crystal and (after minimal exposure for alignment and crystal orientation purposes) collected a data set in two shells (2θ = 5–35° and then 35–40°) at a fast scan rate (8°/min in ω or 16°/min in 2θ with a truncated scan width). Data were corrected for crystal decay (ca. 20%). The

Table II. Final Atomic Coordinates (×10^4) and Equivalent Isotropic Displacement Coefficients (Å^2 × 10^3) for $(\mu\text{-H})_3Ru_3(\mu_3\text{-COMe})(CO)_6\{\mu_3\text{-}(PPh_2CH_2)_3CMe\}$

	x	y	z	U(eq)[a]
Ru(1)	1824 (1)	7067 (1)	8555 (1)	30 (1)
Ru(2)	3524 (1)	6500 (1)	7143 (1)	31 (1)
Ru(3)	2319 (1)	8661 (1)	7515 (1)	30 (1)
H(12)	2493 (40)	6117 (30)	7840 (20)	30
H(23)	3056 (41)	7620 (31)	6824 (21)	31
H(13)	1358 (40)	8232 (30)	8150 (20)	30
P(4)	−534 (2)	6861 (1)	8654 (1)	32 (1)
P(5)	483 (2)	9148 (1)	6896 (1)	31 (1)
P(6)	2151 (2)	5741 (1)	6517 (1)	32 (1)
O(1)	4862 (4)	7513 (3)	8134 (2)	39 (2)
O(11)	3383 (6)	5236 (4)	9278 (3)	75 (2)
O(12)	1186 (6)	8490 (4)	9845 (3)	63 (2)
O(21)	5866 (5)	6922 (5)	5915 (3)	74 (3)
O(22)	5396 (6)	4529 (5)	7557 (3)	88 (3)
O(31)	1674 (7)	10523 (4)	8525 (3)	85 (3)
O(32)	4754 (6)	9476 (4)	6573 (3)	81 (3)
C(11)	2751 (7)	5921 (5)	9013 (3)	44 (3)
C(12)	1426 (7)	7948 (5)	9367 (3)	39 (3)
C(21)	4995 (7)	6759 (6)	6380 (3)	44 (3)
C(22)	4673 (7)	5259 (6)	7400 (3)	47 (3)
C(31)	1931 (7)	9809 (5)	8143 (4)	45 (3)
C(32)	3808 (7)	9181 (5)	6910 (4)	46 (3)
C(1)	3652 (6)	7471 (5)	7940 (3)	31 (2)
C(2)	4720 (8)	8209 (6)	8701 (4)	66 (3)
C(3)	−1302 (6)	7467 (5)	7906 (3)	34 (2)
C(4)	−119 (6)	8027 (4)	6598 (3)	31 (2)
C(5)	260 (6)	6013 (4)	6973 (3)	33 (2)
C(6)	−2040 (6)	7027 (5)	6842 (3)	46 (3)
C(7)	−732 (6)	7139 (5)	7092 (3)	31 (2)
C(411)	−1858 (6)	7610 (5)	9392 (3)	38 (2)
C(412)	−2002 (7)	8715 (6)	9421 (4)	52 (3)
C(413)	−3009 (8)	9297 (7)	9974 (4)	68 (4)
C(414)	−3838 (9)	8809 (8)	10494 (5)	79 (4)
C(415)	−3699 (9)	7760 (8)	10472 (4)	77 (4)
C(416)	−2709 (7)	7140 (6)	9936 (4)	54 (3)
C(421)	−965 (7)	5553 (5)	8772 (3)	39 (2)
C(422)	−68 (8)	4728 (5)	9014 (3)	49 (3)
C(423)	−387 (9)	3739 (6)	9142 (4)	62 (3)
C(424)	−1609 (11)	3554 (6)	9018 (4)	75 (4)
C(425)	−2530 (10)	4364 (7)	8791 (4)	75 (4)
C(426)	−2203 (8)	5361 (6)	8654 (4)	56 (3)
C(511)	1131 (6)	9710 (5)	6004 (3)	34 (2)
C(512)	2355 (7)	9177 (6)	5561 (4)	58 (3)
C(513)	2953 (8)	9600 (7)	4917 (4)	71 (3)
C(514)	2344 (8)	10591 (6)	4720 (4)	59 (3)
C(515)	1103 (9)	11102 (6)	5139 (4)	61 (3)
C(516)	500 (7)	10671 (5)	5774 (3)	50 (3)
C(521)	−1115 (7)	10135 (5)	7264 (3)	36 (2)
C(522)	−977 (10)	11040 (7)	7539 (5)	99 (5)
C(523)	−2132 (14)	11877 (8)	7736 (6)	126 (7)
C(524)	−3463 (10)	11759 (8)	7706 (5)	83 (4)
C(525)	−3555 (9)	10918 (7)	7423 (6)	90 (5)
C(526)	−2421 (9)	10086 (7)	7217 (5)	84 (4)
C(611)	2440 (6)	4289 (5)	6556 (3)	40 (2)
C(612)	2341 (8)	3809 (6)	7220 (4)	62 (3)
C(613)	2531 (11)	2729 (7)	7277 (6)	89 (5)
C(614)	2811 (11)	2115 (7)	6684 (7)	97 (5)
C(615)	2951 (9)	2560 (7)	6023 (6)	83 (5)
C(616)	2750 (7)	3659 (5)	5948 (4)	56 (3)
C(621)	2197 (6)	5985 (5)	5561 (3)	37 (2)
C(622)	1086 (7)	5968 (6)	5263 (3)	49 (3)
C(623)	1151 (8)	6161 (6)	4544 (4)	59 (3)
C(624)	2350 (9)	6358 (7)	4103 (4)	68 (4)
C(625)	3472 (9)	6376 (8)	4372 (4)	79 (4)
C(626)	3407 (8)	6192 (6)	5094 (4)	60 (3)

[a] Equivalent isotropic U defined as one-third of the trace of the orthogonalized U_{ij} tensor.

Table III. Final Atomic Coordinates (×10⁴) and Equivalent Isotropic Displacement Coefficients (Å² × 10³) for $(\mu\text{-H})_2Ru_3(\mu_3\text{-COMe})(CO)_7\{\mu_2\text{-}(PPh_2)_2CH\}\cdot 1.25CH_2Cl_2$

	x	y	z	U(eq)[a]		x	y	z	U(eq)[a]
Ru(1)	7611 (1)	8743 (1)	1879 (1)	42 (1)	C(316)	8635 (9)	8689 (9)	4835 (7)	89 (6)
Ru(2)	6492 (1)	8604 (1)	2254 (1)	42 (1)	C(321)	8635 (7)	6961 (8)	3908 (6)	57 (4)
Ru(3)	6454 (1)	8185 (1)	1153 (1)	48 (1)	C(322)	8392 (7)	6548 (8)	3475 (6)	61 (4)
Ru(4)	2637 (1)	5326 (1)	1878 (1)	43 (1)	C(323)	8547 (8)	5825 (9)	3492 (8)	88 (6)
Ru(5)	1409 (1)	5166 (1)	2070 (1)	44 (1)	C(324)	8940 (9)	5547 (10)	3953 (8)	93 (6)
Ru(6)	1578 (1)	4764 (1)	1031 (1)	49 (1)	C(325)	9193 (9)	5935 (10)	4397 (8)	90 (6)
H(12)	7104 (37)	9211 (42)	2255 (33)	42	C(326)	9079 (8)	6690 (9)	4400 (7)	82 (5)
H(13)	7058 (48)	8877 (51)	1408 (42)	45	C(411)	3863 (6)	4444 (7)	2890 (5)	43 (3)
H(23)	6204 (48)	8714 (52)	1606 (42)	45	C(412)	4427 (6)	4486 (7)	3313 (6)	53 (4)
H(45)	2050 (80)	5657 (93)	1979 (68)	44	C(413)	4901 (8)	3976 (8)	3377 (7)	71 (5)
H(46)	2221 (48)	5465 (52)	1307 (43)	46	C(414)	4798 (8)	3420 (9)	3035 (6)	74 (5)
H(56)	1000 (28)	5213 (41)	1459 (33)	46	C(415)	4245 (8)	3353 (9)	2610 (7)	79 (5)
P(1)	7119 (2)	8516 (2)	3176 (1)	40 (1)	C(416)	3771 (7)	3868 (7)	2539 (6)	58 (4)
P(2)	8330 (2)	8484 (2)	2737 (1)	39 (1)	C(421)	3617 (6)	5834 (6)	3173 (5)	42 (3)
P(3)	8598 (2)	7927 (2)	3911 (2)	52 (2)	C(422)	3473 (7)	6125 (8)	3631 (6)	64 (4)
P(4)	3206 (2)	5086 (2)	2794 (1)	41 (1)	C(423)	3820 (8)	6727 (9)	3880 (7)	82 (5)
P(5)	3261 (2)	4479 (2)	3923 (1)	44 (1)	C(424)	4279 (8)	7019 (10)	3675 (7)	87 (5)
P(6)	1865 (2)	5064 (2)	3027 (1)	39 (1)	C(425)	4442 (8)	6743 (8)	3253 (6)	70 (5)
C(1)	7038 (6)	7910 (7)	1943 (5)	46 (6)	C(426)	4106 (7)	6147 (8)	2981 (6)	66 (4)
C(2)	6792 (7)	6701 (7)	2110 (6)	66 (7)	C(511)	2873 (6)	4637 (7)	4463 (5)	45 (4)
C(3)	7932 (6)	8134 (6)	3257 (5)	38 (5)	C(512)	3083 (7)	5205 (8)	4798 (6)	70 (5)
C(4)	2040 (6)	4475 (7)	1844 (6)	49 (6)	C(513)	2845 (9)	5321 (10)	5261 (8)	95 (6)
C(5)	1783 (7)	3281 (7)	1944 (6)	62 (7)	C(514)	2368 (9)	4899 (10)	5344 (9)	104 (6)
C(6)	2695 (6)	4703 (6)	3214 (5)	42 (5)	C(515)	2163 (8)	4326 (9)	5024 (7)	78 (5)
C(11)	7913 (7)	9700 (8)	1835 (6)	53 (4)	C(516)	2411 (7)	4189 (8)	4580 (6)	59 (4)
C(12)	8176 (7)	8361 (8)	1510 (6)	55 (4)	C(521)	3324 (6)	3517 (7)	3910 (5)	48 (4)
C(21)	5856 (7)	7978 (7)	2360 (6)	51 (4)	C(522)	3612 (8)	3210 (9)	4414 (8)	88 (5)
C(22)	6002 (7)	9414 (8)	2368 (6)	60 (4)	C(523)	3801 (9)	2489 (10)	4432 (8)	100 (6)
C(31)	6024 (8)	8753 (9)	516 (7)	69 (5)	C(524)	3657 (8)	2100 (10)	3971 (7)	83 (5)
C(32)	5782 (8)	7499 (9)	1053 (6)	66 (4)	C(525)	3353 (7)	2410 (8)	3502 (7)	68 (4)
C(33)	6913 (7)	7620 (8)	785 (6)	57 (4)	C(526)	3182 (7)	3090 (7)	3461 (6)	58 (4)
C(41)	3283 (8)	4924 (8)	1585 (7)	64 (4)	C(611)	1887 (6)	5901 (6)	3410 (5)	38 (3)
C(42)	2941 (7)	6291 (9)	1880 (6)	59 (4)	C(612)	1950 (6)	6523 (7)	3142 (6)	48 (4)
C(51)	736 (8)	4549 (8)	2062 (6)	62 (4)	C(613)	1988 (7)	7156 (8)	3435 (6)	67 (4)
C(52)	895 (8)	6005 (9)	2074 (6)	63 (4)	C(614)	1944 (8)	7173 (9)	3959 (7)	77 (5)
C(61)	2082 (7)	4162 (8)	733 (6)	60 (4)	C(615)	1872 (8)	6540 (9)	4207 (7)	78 (5)
C(62)	879 (8)	4124 (9)	852 (7)	65 (4)	C(616)	1856 (6)	5908 (7)	3944 (6)	52 (4)
C(63)	1231 (8)	5366 (8)	373 (7)	66 (4)	C(621)	1413 (6)	4470 (6)	3330 (5)	40 (3)
C(111)	6732 (6)	7929 (7)	3562 (5)	43 (3)	C(622)	1510 (7)	3751 (7)	3317 (6)	54 (4)
C(112)	6240 (7)	8193 (8)	3753 (6)	58 (4)	C(623)	1146 (7)	3258 (9)	3524 (6)	71 (5)
C(113)	5906 (7)	7738 (8)	3999 (6)	65 (4)	C(624)	639 (8)	3538 (9)	3708 (7)	77 (5)
C(114)	6044 (7)	7042 (8)	4043 (6)	62 (4)	C(625)	521 (8)	4232 (8)	3693 (6)	72 (5)
C(115)	6510 (7)	6766 (8)	3821 (6)	64 (4)	C(626)	887 (7)	4717 (8)	3496 (6)	61 (4)
C(116)	6849 (7)	7220 (7)	3580 (6)	57 (4)	O(1)	7265 (4)	7235 (4)	2134 (3)	43 (4)
C(121)	7221 (6)	9338 (7)	3569 (5)	42 (3)	O(4)	2253 (4)	3822 (5)	2057 (3)	49 (4)
C(122)	7262 (7)	9358 (8)	4117 (6)	64 (4)	O(11)	8058 (6)	10256 (6)	1825 (5)	92 (6)
C(123)	7352 (7)	9994 (8)	4399 (7)	70 (5)	O(12)	8507 (5)	8182 (6)	1267 (4)	82 (5)
C(124)	7351 (8)	10630 (10)	4105 (7)	84 (5)	O(21)	5458 (5)	7620 (6)	2412 (5)	83 (5)
C(125)	7291 (7)	10608 (8)	3574 (6)	68 (4)	O(22)	5705 (5)	9881 (5)	2430 (5)	80 (5)
C(126)	7239 (6)	9973 (7)	3275 (6)	52 (4)	O(31)	5802 (7)	9087 (7)	129 (5)	112 (6)
C(211)	8920 (6)	7789 (7)	2748 (5)	43 (3)	O(32)	5373 (6)	7112 (6)	998 (6)	99 (6)
C(212)	8752 (6)	7236 (7)	2385 (5)	48 (4)	O(33)	7206 (6)	7287 (6)	559 (5)	92 (6)
C(213)	9163 (7)	6665 (8)	2423 (6)	63 (4)	O(41)	3652 (6)	4736 (8)	1397 (5)	111 (7)
C(214)	9742 (8)	6664 (9)	2821 (6)	72 (5)	O(42)	3133 (6)	6851 (6)	1916 (4)	89 (5)
C(215)	9933 (7)	7188 (8)	3163 (6)	62 (4)	O(51)	312 (5)	4168 (6)	2042 (4)	85 (5)
C(216)	9520 (7)	7783 (8)	3117 (6)	66 (4)	O(52)	586 (6)	6484 (6)	2023 (5)	93 (6)
C(221)	8831 (6)	9209 (6)	3032 (5)	40 (3)	O(61)	2428 (7)	3815 (6)	584 (5)	99 (6)
C(222)	9276 (7)	9418 (8)	2761 (6)	65 (4)	O(62)	444 (6)	3762 (6)	746 (5)	95 (6)
C(223)	9688 (9)	10008 (10)	2943 (8)	98 (6)	O(63)	1034 (7)	5698 (6)	−6 (5)	106 (6)
C(224)	9610 (8)	10388 (9)	3388 (7)	84 (5)	Cl(71)	9853 (9)	464 (8)	330 (7)	386 (12)
C(225)	9190 (8)	10184 (9)	3673 (7)	80 (5)	C(71)	10089 (28)	854 (30)	−160 (24)	337 (30)
C(226)	8790 (7)	9602 (7)	3486 (6)	53 (4)	Cl(82)	9467 (7)	6004 (7)	737 (5)	301 (9)
C(311)	8349 (7)	8098 (8)	4526 (6)	60 (4)	Cl(81)	9129 (10)	7351 (10)	295 (5)	454 (16)
C(312)	7924 (7)	7691 (8)	4729 (6)	70 (5)	C(81)	9394 (22)	6821 (20)	772 (17)	294 (24)
C(313)	7768 (9)	7893 (11)	5214 (8)	102 (6)	Cl(92)	4383 (5)	2953 (5)	418 (3)	208 (5)
C(314)	8062 (11)	8438 (12)	5475 (10)	122 (7)	Cl(91)	4258 (10)	4384 (7)	136 (5)	373 (13)
C(315)	8475 (10)	8890 (11)	5321 (9)	111 (7)	C(91)	4427 (20)	3815 (19)	538 (15)	268 (19)

[a] Equivalent isotropic U defined as one-third of the trace of the orthogonalized U_{ij} tensor.

data set thus obtained is substantially inferior to those with which we normally work; nevertheless, it enabled the structure to be solved successfully.

Because of the poor quality of the data, only the more significant of the 128 independent non-hydrogen atoms were refined with anisotropic thermal parameters. Nevertheless, the structure was refined to convergence with $R = 5.51\%$ and $R_w = 7.48\%$ for 730 variables refined against those 5264 data with $|F_o| > 6\sigma(|F_o|)$. Not surprisingly, the discrepancy indices for all data are substantially higher: $R = 9.80\%$ and $R_w = 10.66\%$ for all 9358 data.

Further information on the structural analysis is collected in Table I. Final atomic coordinates are given in Table III.

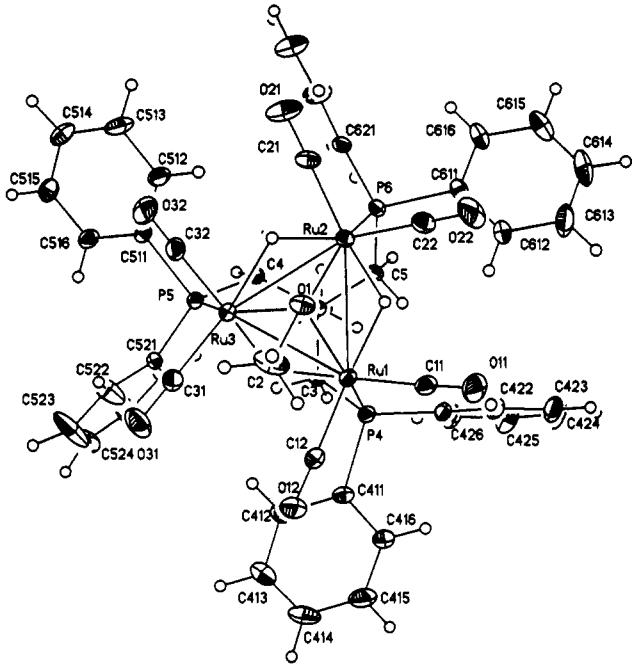

Figure 1. The $(\mu\text{-H})_3Ru_3(\mu_3\text{-COMe})(CO)_6\{\mu_3\text{-}(PPh_2CH_2)_3CMe\}$ molecule viewed approximately down its pseudo-C_3 axis.

Results and Discussion

The substituted clusters $H_3M_3(\mu_3\text{-CX})(CO)_{9-n}L_n$ (M = Ru, X = OMe, Ph, L = $AsPh_3$, PPh_3, n = 1–3;[15] M = Ru, X = NMeBz, L = $SbPh_3$, n = 3;[12] M = Os, X = OMe, L = PPh_3, n = 1, 2;[10] M = Os, X = Me, n = 1[16]) have been previously reported. An X-ray crystallographic study has previously been reported for $H_3Ru_3(CPh)(CO)_7(AsPh_3)_2$,[15] in which the arsine ligands occupy axial positions on two of the three ruthenium centers. The NMR and IR spectral data for all of the triphenylphosphine- and triphenylarsine-substituted clusters show unequivocally that in all cases the EPh_3 ligands are axially coordinated.

$(\mu\text{-H})_3Ru_3(\mu_3\text{-COMe})(CO)_6\{\mu_3\text{-}(PPh_2CH_2)_3CMe\}$. Structure. The crystal consists of discrete molecular units, separated by normal van der Waals distances; there are no abnormally short intermolecular contacts. The molecule has approximate C_3 symmetry (see Figure 1), broken only by a unique site for the pendant –OMe group on the μ_3-COMe ligand and by slight rotations of phenyl groups on the μ_3-$(PPh_2CH_2)_3CMe$ ligand. The molecule is chiral because of the propeller-like arrangements of the phenyl groups; the crystal, however, contains an ordered racemic mixture. Selected interatomic distances appear in Table IV. The three ruthenium atoms are arranged in a triangle (Ru(1)–Ru(2) = 2.860 (1) Å, Ru(2)–Ru(3) = 2.844 (1) Å, Ru(3)–Ru(1) = 2.834 (1) Å; average 2.846 Å) and are capped by a μ_3-COMe ligand with Ru(1)–C(1) = 2.081 (6) Å, Ru(2)–C(1) = 2.068 (6) Å, Ru(3)–C(1) = 2.086 (6) Å, and Ru–C(1)(av) = 2.078 Å; other distances are C(1)–O(1) = 1.369 (8) Å and O(1)–C(2) = 1.405 (9) Å. The opposite face of the Ru_3 triangle is capped symmetrically by a μ_3-$(PPh_2CH_2)_3CMe$ ligand. Important bond lengths are Ru(1)–P(4) = 2.402 (2) Å, Ru(2)–P(6) = 2.413 (2) Å, and Ru(3)–P(5) = 2.392 (2) Å (Ru–P(av) = 2.402 Å). This portion of the molecule is similar to that of $(\mu\text{-H})_4Ru_4(CO)_9\{\mu_3\text{-}(PPh_2)_3CH\}$,[17] except that Ru–P distances are reduced to 2.316 (3)–2.342 (3) Å in this tetranuclear species.

Table IV. Selected Interatomic Distances (Å) for $(\mu\text{-H})_3Ru_3(\mu_3\text{-COMe})(CO)_6\{\mu_3\text{-}(PPh_2CH_2)_3CMe\}$

(A) Ru–Ru, Ru–P, and Ru–H Distances			
Ru(1)–Ru(2)	2.860 (1)	Ru(1)–P(4)	2.402 (2)
Ru(1)–Ru(3)	2.834 (1)	Ru(2)–P(6)	2.413 (2)
Ru(2)–Ru(3)	2.844 (1)	Ru(3)–P(5)	2.392 (2)
Ru(1)–H(12)	1.79 (4)	Ru(2)–H(23)	1.57 (4)
Ru(1)–H(13)	1.69 (4)	Ru(3)–H(13)	1.52 (4)
Ru(2)–H(12)	1.61 (4)	Ru(3)–H(23)	1.84 (4)
(B) Distances Involving the μ_3-COMe Ligand			
Ru(1)–C(1)	2.081 (6)	C(1)–O(1)	1.369 (8)
Ru(2)–C(1)	2.068 (6)	O(1)–C(2)	1.405 (9)
Ru(3)–C(1)	2.086 (6)		
(C) Ru–CO and C–O Distances			
Ru(1)–C(11)	1.875 (7)	C(11)–O(11)	1.148 (9)
Ru(1)–C(12)	1.884 (7)	C(12)–O(12)	1.128 (9)
Ru(2)–C(21)	1.883 (6)	C(21)–O(21)	1.134 (8)
Ru(2)–C(22)	1.886 (7)	C(22)–O(22)	1.138 (9)
Ru(3)–C(31)	1.870 (7)	C(31)–O(31)	1.151 (9)
Ru(3)–C(32)	1.882 (7)	C(32)–O(32)	1.140 (9)
(D) P–C and Capping C–C Distances in the μ_3-$(PPh_2CH_2)_3CMe$ Ligand			
P(4)–C(3)	1.857 (6)	P(5)–C(521)	1.832 (5)
P(4)–C(411)	1.835 (5)	P(6)–C(5)	1.852 (6)
P(4)–C(421)	1.823 (7)	P(6)–C(611)	1.835 (6)
P(5)–C(4)	1.848 (7)	P(6)–C(621)	1.836 (6)
P(5)–C(511)	1.849 (6)		
C(3)–C(7)	1.570 (8)	C(5)–C(7)	1.569 (7)
C(4)–C(7)	1.583 (8)	C(6)–C(7)	1.542 (10)

The six carbonyl ligands occupy equatorial sites, which are all displaced out of the Ru_3 plane and toward the μ_3-COMe ligand. Individual Ru–CO distances range from Ru(3)–C(31) = 1.870 (7) to Ru(2)–C(22) = 1.886 (7) Å (average Ru–CO 1.880 Å), with C–O distances of 1.128 (9)–1.151 (9) Å (average 1.140 Å). The μ-hydride ligands lie out of the Ru_3 plane in the direction of the μ_3-$(PPh_2CH_2)_3CMe$ ligand. The hydride ligands were both located directly and refined. They are associated with the following bond lengths: Ru(1)–H(12) = 1.79 (4) Å and Ru(2)–H(12) = 1.61 (4) Å; Ru(2)–H(23) = 1.57 (4) Å and Ru(3)–H(23) = 1.84 (4) Å; Ru(1)–H(13) = 1.69 (4) Å and Ru(3)–H(13) = 1.52 (4) Å (average Ru–H(bridging) 1.67 Å). Individual angles at the hydride ligands are Ru(1)–H(12)–Ru(2) = 115 (2)°, Ru(2)–H(23)–Ru(3) = 113 (2)°, and Ru(1)–H(13)–Ru(3) = 124 (2)° (average 117°).

$(\mu\text{-H})_3Ru_3(\mu\text{-COMe})(CO)_7\{\mu_2\text{-}(PPh_2)_3CH\}\cdot 1.25CH_2Cl_2$. Structure. The crystallographic asymmetric unit consists of two $(\mu\text{-H})_3Ru_3(\mu\text{-COMe})(CO)_7\{\mu_2\text{-}(PPh_2)_3CH\}$ molecules and 2.5 CH_2Cl_2 molecules (the half-unit of which is half of a partially disordered molecule at the origin). The individual molecules are separated by normal van der Waals distances, with no abnormally short intermolecular contacts.

This structural study is of lower accuracy than the previous one, due to the need to collect data rapidly (before catastrophic crystal decomposition occurred).

Selected interatomic distances are collected in Table V. The two cluster molecules are essentially identical. The core of one such molecule is shown in Figure 2. In subsequent discussions the interatomic parameters for the molecule based on the Ru(1)–Ru(2)–Ru(3) core will be discussed; the equivalent parameters for the molecule based on the Ru(4)–Ru(5)–Ru(6) core will follow in parentheses.

(15) Rahman, Z. A.; Beanan, L. R.; Bavaro, L. M.; Modi, S. P.; Keister, J. B.; Churchill, M. R. *J. Organomet. Chem.* **1984**, *263*, 75.
(16) Brown, S. C.; Evans, J. *J. Chem. Soc., Dalton Trans.* **1982**, 1049.
(17) Bahsoun, A. A.; Osborn, J. A.; Kintzinger, J.-P.; Bird, P. H.; Siriwardane, U. *Nouv. J. Chim.* **1984**, *8*, 125.
(18) $^{13}C\{^1H\}$ NMR for $H_3Ru_3(COMe(CO)_6(PPh_3)_3$ ($CDCl_3$): 253.9 (q, 1 C, J_{PC} = 39 Hz, μ_3-C), 196.4 (s, 6 C, equatorial CO's), 128–138 (phenyl), 66.4 (s, 1 C, OCH_3) ppm.
(19) Balavoine, G.; Collin, J.; Bonnet, J. J.; Lavigne, G. *J. Organomet. Chem.* **1985**, *280*, 429.

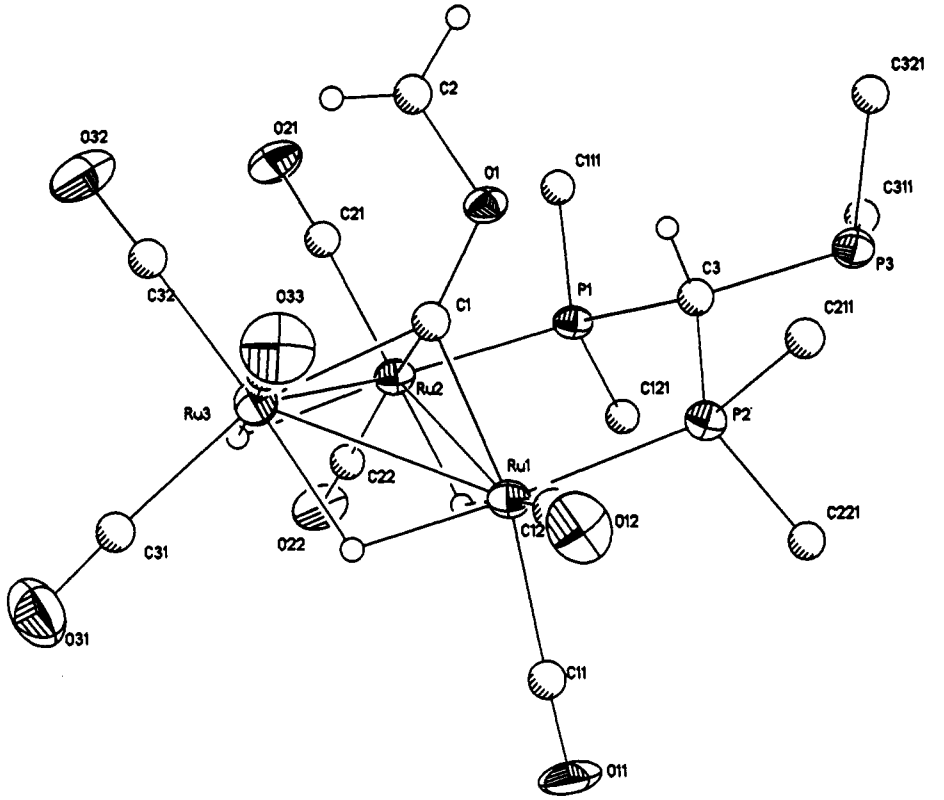

Figure 2. The core of one metal cluster unit in $(\mu\text{-H})_3Ru_3(\mu_3\text{-COMe})(CO)_7\{\mu_2\text{-}(PPh_2)_3CH\}\cdot 1.25CH_2Cl_2$.

The three ruthenium atoms are arranged in a triangle with Ru(1)–Ru(2) = 2.854 (2) Å Ru(2)–Ru(3) = 2.870 (2) Å and Ru(3)–Ru(1) = 2.854 (2) Å (Ru(4)–Ru(5) = 2.851 (2) Å, Ru(5)–Ru(6) = 2.852 (2) Å, and Ru(6)–Ru(4) = 2.858 (2) Å). The μ_3-COMe ligand caps the Ru_3 triangle with Ru(1)–C(1) = 2.050 (14) Å, Ru(2)–C(1) = 2.074 (14) Å and Ru(3)–C(1) = 2.099 (12) Å (Ru(4)–C(4) = 2.061 (14 Å, Ru(5)–C(4) = 2.090 (15) Å and Ru(6)–C(4) = 2.082 (13) Å). The $HC(PPh_2)_3$ moiety acts only as a bidentate (rather than tridentate) ligand and spans *equatorial* sites on adjacent ruthenium atoms, with Ru(1)–P(2) = 2.328 (3) Å and Ru(2)–P(1) = 2.342 (3) Å (Ru(4)–P(4) = 2.332 (3) Å and Ru(5)–P(6) = 2.342 (4) Å). It is possible that radiation damage to this material results from some combination of solvent loss, CO loss, and intermolecular coordination of the free pendant $-PPh_2$ group based upon P(3) (P(5)).

The hydride ligands were located and refined. Esd's associated with Ru–H distances are very large, and values range from 1.45 (9) to 1.87 (9) Å, averaging 1.71 Å (1.49 (9)–2.06 (9) Å, averaging 1.71 Å).

Axial vs Equatorial Coordination. Substitutional preferences for the clusters $(\mu\text{-H})_3M_3(\mu_3\text{-E})(CO)_{9-n}L_n$ have recently been examined.[20] The clusters $H_3Ru_3(\mu_3\text{-Bi})(CO)_{9-n}L_n$ (L = PEt_3, $P(OMe)_3$) exist in solution as equilibrium mixtures of axially and equatorially substituted metal centers.[20] For $H_3Ru_3(\mu_3\text{-CX})(CO)_{9-n}L_n$ axial substitution has been demonstrated for larger ligands (e.g. $H_3Ru_3(COMe)(CO)_7(AsPh_3)_2$), but equatorial substitution is found for small ligands (e.g. $H_3Ru_3(CPh)(CO)_8L$; L = pyridine, NCMe).[21] As noted by Johnson, Lewis, and Whitton,[20] as the bond lengths between M and the capping atom E in these structures increase, the angle between the M–L(axial) bond and the M_3 plane decreases, and the steric interactions between axial ligands across the M_3 face increase. Thus, for unidentate ligands the axial–equatorial substitution pattern is governed primarily by steric interactions.

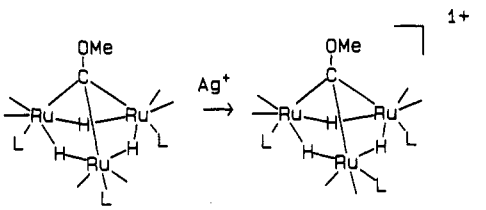

Figure 3. Proposed isomerization for $[H_3Ru_3(\mu_3\text{-COMe})(CO)_6(PPh_3)_3]^+$.

Equatorial substitution in $H_3Ru_3(COMe)(CO)_7\{(PPh_2)_3CH\}$ is undoubtedly due to the small "bite" of the chelating ligand. The "ideal" angle θ between the Ru–L(axial) bonds and the Ru_3 plane should be ca. 120° (for $H_3Ru_3(\mu_3\text{-}CC_6H_4Me)(CO)_9$, θ = 122° to the axial CO ligands,[22] and for $H_3Ru_3(CPh)(CO)_7(AsPh_3)_2$ the angle θ to the axial $AsPh_3$ ligands is 124°.[15] For face capping by the $(PPh_2)_3CH$ ligand a much smaller angle is required. For the substituted derivatives $M_4(\mu\text{-CO})_3(CO)_6\{\mu_3\text{-}(PPh_2)_3CH\}$ (M = Co,[23] Rh,[24] Ir[25]) and $H_4Ru_4(CO)_9\{\mu_3\text{-}(PPh_2)_3CH\}$[17] the longer M–M bonds to the capping $M(CO)_3$ unit make the angle between the M–L(axial) bonds and the M_3 face smaller, and therefore, the $(PPh_2)_3CH$ ligand can span the M_3 face. For example, θ is only 95° in $H_4Ru_4(CO)_9\{\mu_3\text{-}(PPh_2)_3CH\}$.

(20) Johnson, B. F. G.; Lewis, J.; Whitton, A. J. *J. Chem. Soc., Dalton Trans.* **1990**, 3129.
(21) Beanan, L. R. Ph.D. Thesis, State University of New York at Buffalo, Buffalo, NY, 1986.
(22) Churchill, M. R.; Duggan, T. P.; Keister, J. B.; Ziller, J. W. *Acta Crystallogr.* **1987**, *C43*, 203.
(23) (a) Darensbourg, D. J.; Zalewski, D. J.; Delord, T. *Organometallics* **1984**, *3*, 1210. (b) Darensbourg, D. J.; Zalewski, D. J.; Rheingold, A. L.; Durney, R. L. *Inorg. Chem.* **1986**, *25*, 3281. (c) Bahsoun, A. A.; Osborn, J. A.; Voelker, C.; Bonnet, J.-J.; Lavigne, G. *Organometallics* **1982**, *1*, 1114.
(24) Kennedy, J. R.; Selz, P.; Rheingold, A. L.; Trogler, W. C.; Basolo, F. *J. Am. Chem. Soc.* **1989**, *111*, 3615.
(25) Clucas, J. A.; Harding, M. M.; Nicholls, B. S.; Smith, A. K. *J. Chem. Soc., Chem. Commun.* **1984**, 319.

Table V. Selected Interatomic Distances (Å) for $(\mu\text{-H})_3Ru_3(\mu_3\text{-COMe})(CO)_7\{\mu_3\text{-}(PPh_2)_3CH\}\cdot 1.25CH_2Cl_2$

(A) Ru–Ru, Ru–P, and Ru–H Distances			
Ru(1)–Ru(2)	2.854 (2)	Ru(4)–Ru(5)	2.851 (2)
Ru(1)–Ru(3)	2.854 (2)	Ru(4)–Ru(5)	2.858 (2)
Ru(2)–Ru(3)	2.870 (2)	Ru(5)–Ru(6)	2.852 (2)
Ru(1)–P(2)	2.328 (3)	Ru(4)–P(4)	2.332 (3)
Ru(2)–P(1)	2.342 (3)	Ru(5)–P(6)	2.342 (4)
Ru(1)–H(12)	1.87 (9)	Ru(4)–H(45)	1.51 (18)
Ru(1)–H(13)	1.45 (9)	Ru(4)–H(46)	1.49 (10)
Ru(2)–H(12)	1.76 (8)	Ru(5)–H(45)	1.74 (18)
Ru(2)–H(23)	1.59 (10)	Ru(5)–H(56)	1.54 (8)
Ru(3)–H(13)	1.84 (9)	Ru(6)–H(46)	1.91 (9)
Ru(3)–H(23)	1.72 (11)	Ru(6)–H(56)	2.06 (9)
(B) Distances Involving the μ_3-COMe Ligand			
Ru(1)–C(1)	2.050 (14)	Ru(4)–C(4)	2.061 (14)
Ru(2)–C(1)	2.074 (14)	Ru(5)–C(4)	2.090 (15)
Ru(3)–C(1)	2.099 (12)	Ru(6)–C(4)	2.082 (13)
C(1)–O(1)	1.414 (15)	C(4)–O(4)	1.383 (16)
O(1)–C(2)	1.432 (17)	O(4)–C(5)	1.420 (16)
(C) Ru–CO and C–O Distances			
Ru(1)–C(11)	1.953 (16)	Ru(4)–C(41)	1.920 (18)
Ru(1)–C(12)	1.886 (17)	Ru(4)–C(42)	1.954 (16)
Ru(2)–C(21)	1.900 (15)	Ru(5)–C(51)	1.870 (17)
Ru(2)–C(22)	1.942 (16)	Ru(5)–C(52)	1.953 (17)
Ru(3)–C(31)	1.942 (16)	Ru(6)–C(61)	1.884 (17)
Ru(3)–C(32)	1.919 (17)	Ru(6)–C(62)	1.897 (17)
Ru(3)–C(33)	1.883 (17)	Ru(6)–C(63)	1.983 (16)
C(11)–O(11)	1.108 (19)	C(41)–O(41)	1.100 (23)
C(12)–O(12)	1.119 (21)	C(42)–O(42)	1.141 (20)
C(21)–O(21)	1.136 (19)	C(51)–O(51)	1.160 (20)
C(22)–O(22)	1.136 (20)	C(52)–O(52)	1.118 (20)
C(31)–O(31)	1.150 (20)	C(61)–O(61)	1.141 (22)
C(32)–O(32)	1.129 (21)	C(62)–O(62)	1.136 (20)
C(33)–O(33)	1.155 (21)	C(63)–O(63)	1.124 (20)
(D) P–C Distances in the μ_2-$(PPh_2)_3CH$ Ligand			
P(1)–C(3)	1.862 (13)	P(4)–C(6)	1.886 (15)
P(1)–C(111)	1.837 (15)	P(4)–C(411)	1.840 (13)
P(1)–C(121)	1.834 (13)	P(4)–C(421)	1.804 (12)
P(2)–C(3)	1.885 (14)	P(5)–C(6)	1.906 (11)
P(2)–C(211)	1.835 (13)	P(5)–C(511)	1.819 (15)
P(2)–C(221)	1.783 (12)	P(5)–C(521)	1.842 (14)
P(3)–C(3)	1.897 (11)	P(6)–C(6)	1.854 (13)
P(3)–C(311)	1.811 (17)	P(6)–C(611)	1.860 (13)
P(3)–C(321)	1.843 (15)	P(6)–C(621)	1.805 (14)

On the other hand, no M_3 face-capped complexes of $(PPh_2CH_2)_3CMe$ have been structurally characterized previously. In this case, the larger "bite" afforded by the methylene bridges allows for face capping (θ = 113°) on the $H_3Ru_3(\mu_3\text{-COMe})(CO)_6$ unit, although ring strain makes the chelated cluster less stable than $H_3Ru_3(COMe)(CO)_6(PPh_3)_3$.

One-Electron Oxidation of $H_3Ru_3(COMe)(CO)_7\{(PPh_2CH_2)_3CMe\}$. While $H_3Ru_3(COMe)(CO)_6(PPh_3)_3$ has equivalent, axially coordinated phosphine ligands, the analogous 47-electron cation displays an EPR spectrum in which the unpaired electron is coupled to only two inequivalent ^{31}P nuclei. We had proposed that the structure of the cation contained one equatorially coordinated and two axially coordinated PPh_3 ligands (Figure 3), but alternative isomerizations involving hydride and/or COMe migrations were also possible. We sought to resolve this question by preparing the 47-electron derivative $[H_3Ru_3(COMe)(CO)_6\{(PPh_2CH_2)_3CMe\}]^+$, in which chelation prevents axial–equatorial ligand isomerization.

Cyclic voltammograms of $H_3Ru_3(COMe)(CO)_7(PPh_3)_2$ and $H_3Ru_3(COMe)(CO)_6(PPh_3)_3$ show quasi-reversible, one-electron oxidations at 0.51 and 0.31 V, respectively; at more extreme potentials each displays an irreversible one-electron oxidation. Substitution of each phosphine ligand for a carbonyl decreases the oxidation potential by approximately 150–200 mV per ligand.[10]

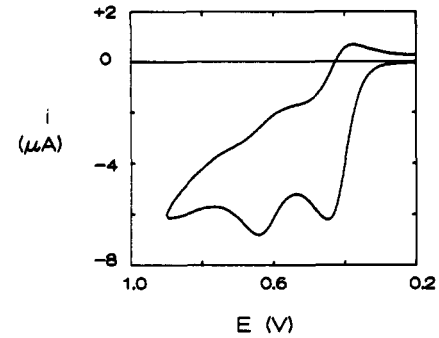

Figure 4. Cyclic voltammogram of $(\mu\text{-H})_3Ru_3(\mu_3\text{-COMe})(CO)_6\{\mu_3\text{-}(PPh_2CH_2)_3CMe\}$ in dichloromethane (0.1 M tetrabutylammonium tetrafluoroborate) at a scan rate of 100 mV/s. The reference electrode is the SCE.

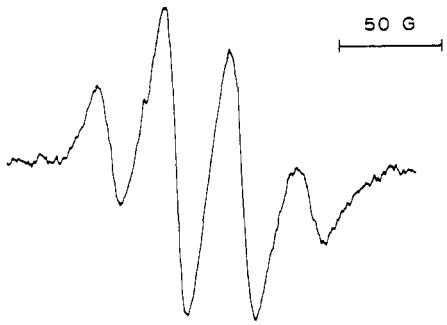

Figure 5. EPR spectrum of $[(\mu\text{-H})_3Ru_3(\mu_3\text{-COMe})(CO)_6\{\mu_3\text{-}(PPh_2CH_2)_3CMe\}]^+$ in dichloromethane.

On the basis of the structural analogy and electronically similar ligand characteristics the electrochemical behavior of $H_3Ru_3(COMe)(CO)_6\{(PPh_2CH_2)_3CMe\}$ was expected to be very similar to that of $H_3Ru_3(COMe)(CO)_6(PPh_3)_3$. The cyclic voltammogram (Figure 4, 100 mV/s) does display a quasi-reversible one-electron oxidation at $(E_{p,a} + E_{p,c})/2$ = 0.42 V and an irreversible, one-electron oxidation at $E_{p,a}$ = 0.63 V, but these potentials are significantly more positive than would be expected on the basis of the donor ability of the ligand. Furthermore, the first oxidation is less reversible (ΔE_p = 81 mV, $i_{p,c}/i_{p,a}$ = 0.60) than that of $H_3Ru_3(COMe)(CO)_6(PPh_3)_3$ (ΔE = 117 mV, $i_{p,a}/i_{p,c}$ = 0.77),[10] presumably due to a smaller heterogeneous electron-transfer rate constant or instability of the oxidation product.

Treatment of the orange solution of $H_3Ru_3(COMe)(CO)_6\{(PPh_2CH_2)_3CMe\}$ in dichloromethane with $AgSO_3CF_3$ produces a green solution, indicative of the formation of a radical cation. Consistent with the electrochemical data, $[H_3Ru_3(COMe)(CO)_6\{(PPh_2CH_2)_3CMe\}]^+$ decomposes much more quickly (within minutes) than does $[H_3Ru_3(COMe)(CO)_6(PPh_3)_3]^+$.[10] The EPR spectrum, recorded at 200 K (Figure 5), indicates that the electron is coupled equivalently to all three phosphorus atoms (g = 2.07 (q), A = 32.6 G). The hyperfine coupling constant (32.6 G) is similar to those noted earlier for $[H_3Ru_3(CNMeBz)(CO)_6(PPh_3)_3]^+$ (36.3 G) and $[H_3Ru_3(COMe)(CO)_7(PPh_3)_2]^+$ (51.1 G), and the two inequivalent hyperfine coupling constants of $[H_3Ru_3(COMe)(CO)_6(PPh_3)_3]^+$ (40.4 and 59.8 G).[10] We conclude that the EPR spectrum of $[H_3Ru_3(COMe)(CO)_6(PPh_3)_3]^+$ is indicative of a structure with two axial and one equatorial PPh_3 ligand and *not* of a structure containing an unsymmetrical arrangement of hydride or COMe ligands. MO calculations on $H_3Ru_3(CX)(CO)_9$ (X = H, Cl, Br) by Sherwood and Hall[26] in-

(26) Sherwood, D. E., Jr.; Hall, M. B. *Organometallics* **1982**, *1*, 1519.

dicate that the HOMO of the 48-electron precursor should be largely Ru–μ_3-C bonding in character, localized trans to the Ru–L(axial) bonds. The coupling constant to the equatorial ^{31}P nucleus, cis to the Ru–COMe bond, must be too small to be resolved (cf. the ^{31}P–$^{13}COMe$ J_{trans} value of 39 Hz in $H_3Ru_3(COMe)(CO)_6(PPh_3)_3$[18] vs J_{cis} = 3.5 Hz in $H_3Ru_3(COMe)(CO)_7\{(PPh_2)_3CH\}$).

Acknowledgment. Purchase of a Siemens R3m/V diffractometer was made possible by a grant from the Chemical Instrumentation Program of the National Science Foundation (Grant No. 89-13733). This work was supported by the National Science Foundation through Grant No. CHE8900921 (J.B.K.). We thank Professor Robert D. Allendoerfer for assistance with the EPR measurements.

Supplementary Material Available: Tables of distances and angles, anisotropic thermal parameters, and calculated positions of H atoms for $(\mu\text{-H})_3Ru_3(\mu_3\text{-COMe})(CO)_6\{\mu_3\text{-}(PPh_2CH_2)_3CMe\}$ and $(\mu\text{-H})_3Ru_3(\mu_3\text{-COMe})(CO)_7\{\mu_2\text{-}(PPh_2)_3CH\}\cdot 1.25CH_2Cl_2$ (14 pages); tables of F_o/F_c values (56 pages). Ordering information is given on any current masthead page.

Pentadienyl–Iridium–Phosphine Chemistry.[1] Survey of the Reactions of Pentadienide Reagents with $ClIrL_3$ Complexes

John R. Bleeke,* Devran Boorsma, Michael Y. Chiang, Thomas W. Clayton, Jr.,† Tesfamichael Haile, Alicia M. Beatty, and Yun-Feng Xie

Department of Chemistry, Washington University, St. Louis, Missouri 63130

Received January 22, 1991

A systematic study of the reactions of four $ClIrL_3$ complexes with pentadienide reagents has been carried out. Treatment of $ClIr(PEt_3)_3$ with potassium pentadienide produces (1,4,5-η-pentadienyl)$Ir(PEt_3)_3$ (**2**), while the reaction of $ClIr(PMe_3)_3$ with potassium pentadienide yields the analogous trimethylphosphine compound **5**. In contrast, treatment of $ClIr(PMe_3)_3$ with potassium 2,4-dimethylpentadienide produces an equilibrium mixture of (1,4,5-η-2,4-dimethylpentadienyl)$Ir(PMe_3)_3$ (**3**) and the metallacyclohexadiene complex *fac*-$(IrCH_2C(Me)=CHC(Me)=CH)(PMe_3)_3(H)$ (**4**). The formation of **4** involves the intermediacy of 16e$^-$ (η^1-2,4-dimethylpentadienyl)$Ir(PMe_3)_3$, which intramolecularly activates a C–H bond on the end of the pentadienyl chain. Vaska's complex, $ClIr(PPh_3)_2(CO)$, reacts with potassium 2,4-dimethylpentadienide to produce an equilibrium mixture of (1,4,5-η-2,4-dimethylpentadienyl)$Ir(PPh_3)_2(CO)$ (**6**) and (1–3-η-2,4-dimethylpentadienyl)$Ir(PPh_3)_2(CO)$ (**7**). The analogous reaction involving unmethylated pentadienide produces exclusively (1–3-η-pentadienyl)$Ir(PPh_3)_2(CO)$ (**8**). This species undergoes a dynamic process in solution, which involves shuttling between η^3- and η^1-pentadienyl bonding modes. Treatment of $ClIr(PEt_3)_2(CO)$ with potassium 2,4-dimethylpentadienide yields (1,4,5-η-2,4-dimethylpentadienyl)$Ir(PEt_3)_2(CO)$ (**9**), while the analogous reaction involving unmethylated pentadienide produces an equilibrium mixture of (1,4,5-η-pentadienyl)$Ir(PEt_3)_2(CO)$ (**10**) and (1–3-η-pentadienyl)$Ir(PEt_3)_2(CO)$ (**11**). Molecular structures of compounds **2**, **3**, **6**, and **8** have been determined by single-crystal X-ray diffraction studies. Crystal structure data for these compounds are as follows: **2**, monoclinic, $P2_1/c$, a = 15.489 (5) Å, b = 11.453 (5) Å, c = 15.769 (4) Å, β = 101.83 (2)°, V = 2738 (2) Å^3, Z = 4, R = 0.038 for 3572 reflections with $I > 3\sigma(I)$; **3**, monoclinic, $P2_1/n$, a = 8.958 (6) Å, b = 20.308 (5) Å, c = 11.970 (5) Å, β = 93.14 (5)°, V = 2174 (2) Å^3, Z = 4, R = 0.037 for 3440 reflections with $I > 3\sigma(I)$; **6**, monoclinic, $P2_1/n$, a = 13.518 (5) Å, b = 17.862 (6) Å, c = 15.417 (5) Å, β = 93.59 (3)°, V = 3715 (2) Å^3, Z = 4, R = 0.035 for 5003 reflections with $I > 3\sigma(I)$; **8**, monoclinic, $P2_1/c$, a = 17.276 (7) Å, b = 23.038 (8) Å, c = 18.896 (5) Å, β = 111.92 (2)°, V = 6977 (4) Å^3, Z = 8, R = 0.049 for 6353 reflections with $I > 3\sigma(I)$.

Introduction

In an earlier paper,[2] we reported that $ClIr(PEt_3)_3$ reacts with potassium 2,4-dimethylpentadienide to produce a novel iridacyclohexadiene complex, $(IrCH_2C(Me)=CHC(Me)=CH)(PEt_3)_3(H)$ (**1**). This reaction proceeds through the intermediacy of 16e$^-$ (η^1-2,4-dimethylpentadienyl)$Ir(PEt_3)_3$, which undergoes intramolecular oxidative addition across an sp^2 C–H bond on the dangling terminus of the pentadienyl ligand. Compound **1** is the parent to a large family of unsaturated six-membered metallacycles,[2] including a rare metallabenzene complex $(Ir{-}CH{=}C(Me){-}CH{=}C(Me){-}CH)(PEt_3)_3$.[3]

Scheme I

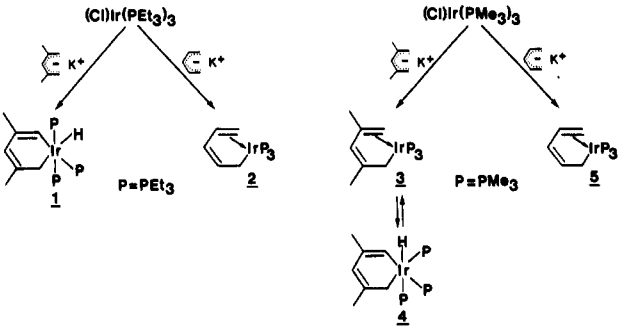

In order to probe the generality of this novel synthetic route to unsaturated six-membered metallacycles and to

† Pew Postdoctoral Fellow.

0276-7333/91/2310-2391$02.50/0